DALTON
FULL PAPER

Synthesis and structural study of late transition metal complexes of *N*-[(diphenylphosphino)methyl]-2-pyridinamine and *N*-cyclohexyl-*N*-[(diphenylphosphino)methyl]-2-pyridinamine

Hai-Bin Song,[a] **Zheng-Zhi Zhang**[b] **and Thomas C. W. Mak** *[a]

[a] *Department of Chemistry, The Chinese University of Hong Kong, Shatin, New Territories, Hong Kong SAR, P. R. China. E-mail: tcwmak@cuhk.edu.hk*
[b] *State Key Laboratory of Elemento-Organic Chemistry, Nankai University, Tianjin, P. R. China*

Received 9th October 2001, Accepted 23rd January 2002
First published as an Advance Article on the web 7th March 2002

The reaction of *N*-[(diphenylphosphino)methyl]-2-pyridinamine and *N*-cyclohexyl-*N*-[(diphenylphosphino)methyl]-2-pyridinamine with palladium(II), copper(I) and silver(I) salts and iron pentacarbonyl in different stoichiometric ratios yielded a series of complexes that display various coordination modes, including a novel P,N(amine),-N(pyridyl)-bridging mode in a dinuclear silver complex which is consolidated by the argentophilic interaction.

Introduction

There has been continuing interest in the synthesis and chemistry of hemilabile ligands in view of their wide use in coordination, organometallic and catalyst chemistry.[1] Pyridine-phosphine ligands, which contain a soft Lewis base (the phosphorus atom) and a hard Lewis base (the nitrogen atom), have attracted particular attention in recent years,[2] as the electronic differentiation of these donor atoms helps to stabilise various types and oxidation states of metals. One prominent example is 2-(diphenylphosphino)pyridine, Ph_2Ppy, which displays several ligation modes to transition metals: P-coordination, N-coordination, P,N-chelating and P,N-bridging,[3] generating complexes that exhibit different spectroscopic properties, reactivities and applications. The functionalisation of pyridine-phosphines can lead to enhancement in catalytic reactivity.[4] For instance, higher activity and selectivity is exhibited by the substituted ligand system **I** relative to Ph_2Ppy in the palladium-catalysed carbonylation of alkynes,[4f–g] and by **II** relative to $Ph_2P(3\text{-py})$ in the rhodium-catalysed hydroformylation of 1-octene.[4h] Furthermore, the introduction of methoxy groups in the 2- and 6-positions in **III** facilitates the rhodium-catalysed hydrogenation of olefins, whereas the parent pyridylphosphine complexes are inactive.[4j]

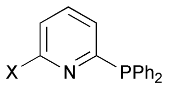

I

X = Me, Br, OMe

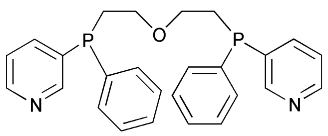

II

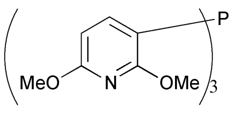

III

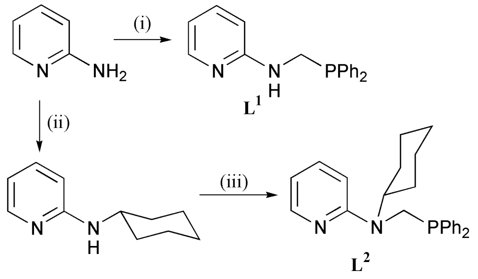

Scheme 1 Reagents: (i) Ph_2PCH_2OH; (ii) H_2SO_4, $C_6H_{11}OH$; (iii) Ph_2PH, $(CH_2O)_n$.

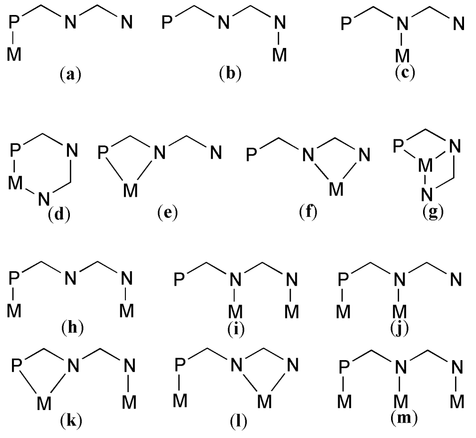

Scheme 2 Possible coordination modes of phosphinopyridinamine ligands.

The functionalised pyridinamine ligands *N*-[(diphenylphosphino)methyl]-2-pyridinamine (L^1)[5a] and *N*-cyclohexyl-*N*-[(diphenylphosphino)methyl]-2-pyridinamine (L^2)[5b] were prepared recently according to Scheme 1. The possible coordination modes of this kind of ligands are shown in Scheme 2. The P,N(pyridyl)-chelating coordination mode (**d**) of L^1 and the P,N(pyridyl)-bridging mode (**h**) of L^2 have been substantiated in previous works.[5]

Herein, we react L^1 and L^2 with iron pentacarbonyl and palladium(II), copper(I) and silver(I) salts in different stoichiometric ratios to form a series of complexes in which the ligands adopt a variety of new coordination modes, namely the

DOI: 10.1039/b109191n

P-coordinating (**a**) and P,N(pyridyl)-bridging (**h**) of L^1 and P,N(pyridyl)-chelating (**d**) modes, and a novel P,N(amine),-N(pyridyl)-bridging mode (**l**) of L^2, as determined from the X-ray structures of these compounds.

Experimental

General

Unless otherwise stated, all reactions were performed under a nitrogen atmosphere using Schlenk techniques. The solvents were purified by standard methods. Infrared spectra were recorded on a Nicolet Impact 420 FT-IR spectrometer from KBr discs. Ligands L^1 and L^2 were prepared by literature methods.[5]

CAUTION! While none of the perchlorate complexes proved to be shock sensitive, appropriate precautions should always be taken when working with them.

Preparations

[$Ph_2P(O)CH_2NH(C_5H_5N)$]ClO_4, 1. 0.08 g (0.27 mmol) L^1 and 0.1 g (0.27 mmol) [$Co(H_2O)_6$]$(ClO_4)_2$ were mixed in 10 cm^3 CH_3CN in air and the solution was stirred overnight. The solution was concentrated and addition of diethyl ether gave colorless crystals of **1** in 50% yield. Found: C, 52.83; H, 4.44; N, 6.63; calc. for $C_{18}H_{18}N_2O_4PCl$: C, 52.89; H, 4.44; N, 6.85%.

***trans*-Fe(CO)$_3$(L^1)$_2$, 2.** This compound was prepared by the published procedure for *trans*-$Fe(CO)_3(PR_3)_2$[6] and single crystals were recrystallised from CH_2Cl_2–CH_3OH. Yield 60%. Found: C, 64.51; H, 4.72; N, 7.83; calc. for $C_{39}H_{34}N_4O_3P_2Fe$: C, 64.65; H, 4.73; N, 7.73%. IR ν(CO): 1880 cm^{-1}.

[Pd(L^1)$_2$](ClO_4)$_2$, 3. To a stirred solution of 0.2 g (0.68 mmol) of L^1 in 10 cm^3 of CH_2Cl_2 was added 0.1 g (0.34 mmol) of Na_2PdCl_4 at ambient temperature. After stirring the solution for *ca.* 30 min, the precipitated NaCl was filtered off and to the clear filtrate was added $TlClO_4$ (0.21 g, 0.34 mmol). After stirring the yellow solution for 30min, the white precipitate of TlCl was filtered off and the filtrate concentrated *in vacuo* to *ca.* 2 cm^3. Subsequent diethyl ether diffusion into the solution afforded yellow crystals of **3** in 80% yield. Found: C, 48.65; H, 3.86; N, 6.29; calc. for $C_{36}H_{34}N_4O_8P_2Cl_2Pd$: C, 48.58; H, 3.85; N, 6.30%.

[$PdCl_2$(μ-L^1)]$_2$, 4. 0.1 g (0.34 mmol) L^1 and 0.1 g (0.34 mmol) Na_2PdCl_4 were mixed in 10 cm^3 CH_2Cl_2 and the solution was stirred for 20 min. The undissolved material was filtered off and the filtrate was concentrated *in vacuo* to *ca.* 2 cm^3. Diffusion of ethanol into this solution gave yellow crystals of **4**·$2CH_2Cl_2$ in 65% yield. Found: C, 46.12; H, 3.61; N, 5.80; calc. for $C_{18}H_{17}N_2PCl_2Pd$: C, 46.04; H, 3,65; N, 5.97%.

[Cu(L^1)$_2$]ClO_4, 5. 0.1 g (0.3 mmol) [$Cu(CH_3CN)_4$]ClO_4 was dissolved in 5 cm^3 CH_3CN and a solution of 0.19 g (0.65 mmol) L^1 in 5 cm^3 CH_2Cl_2 was added with stirring. The reaction mixture stirred for 20 min and concentrated *in vacuo* to *ca.* 2 cm^3. Subsequent diethyl ether diffusion into the solution afforded colorless crystals of **5** in 85% yield. Found: C, 59.67; H, 4.54; N, 7.47; calc. for $C_{36}H_{34}N_4O_4P_2ClCu$: C, 59.83; H, 4.58; N, 7.50%.

[Ag(μ-L^1)(CH_3CN)]$_n$(ClO_4)$_n$, 6. 0.1 g (0.48 mmol) $AgClO_4$ was dissolved in 5 cm^3 CH_3CN and a solution of 0.14 g (0.48 mmol) L^1 in 5 cm^3 CH_3CN was added with stirring. After stirring for 20 min, the solution was concentrated *in vacuo* to *ca.* 2cm^3 and then diethyl ether added to give colorless crystals of **6** in 60% yield. Found: C, 44.13; H, 3.69; N, 7.57; calc. for $C_{20}H_{20}N_3O_4PClAg$: C, 44.43; H, 3.73; N, 7.77%.

[Ag(L^1)$_2$(2-Py-NH_2)]ClO_4, 7. 0.29 g (1 mmol) L^1, 0.1 g (0.48 mmol) $AgClO_4$ and 0.045 g (0.48 mmol) 2-aminopyridine were added to 10 cm^3 CH_3CN. The mixture was stirred for 10 min, then the solution was concentrated to 2 cm^3 and diethyl ether was diffused into it to give colorless crystals of **7**·CH_3CN in 50% yield. Found: C, 55.20; H, 4.65; N, 9.60; calc. for $C_{41}H_{40}N_6O_4P_2ClAg$: C, 55.58; H, 4.55; N, 9.49%.

Pd(L^2)Cl_2, 8. 0.13 g (0.34 mmol) L^2 and 0.1 g (0.34 mmol) Na_2PdCl_4 was mixed together in 10 cm^3 CH_2Cl_2. The solution was stirred for 20 min and then filtered to remove undissolved material. The solution was concentrated *in vacuo* to *ca.* 1–2 cm^3 and then EtOH diffused into the solution to afford yellow crystals of **8**. Found: C, 52.49; H, 4.97; N, 5.05; calc. for $C_{24}H_{27}N_2PCl_2Pd$: C, 52.24; H, 4.93; N, 5.08%.

[Cu(L^2)$_2$]ClO_4, 9. 0.1 g (3 mmol) [$Cu(CH_3CN)_4$]ClO_4 was added to a solution of 0.11 g (0.3 mmol) L^2 in CH_2Cl_2 (10 cm^3) and the mixture was stirred until all the [$Cu(CH_3CN)_4$]ClO_4 dissolved. Then, the clear solution was concentrated *in vacuo* to *ca.* 2 cm^3 and slow diffusion of diethyl ether into it gave colorless single crystals of **9** suitable for X-ray analysis in 85% yield. Found: C, 62.99; H, 5.97; N, 6.05; calc. for $C_{48}H_{54}N_4O_4P_2ClCu$: C, 63.22; H, 5.97; N, 6.15%.

Ag(L^2)ClO_4, 10. 0.1 g (0.48 mmol) $AgClO_4$ and 0.18 g (0.48 mmol) L^2 were mixed in 10 cm^3 CH_3CN–CH_2Cl_2 (1 : 1) with stirring. After all the $AgClO_4$ had dissolved, the solution was concentrated *in vacuo* to *ca.* 2cm^3 and diethyl ether diffused into it to give needle-like microcrystals of **10** in 80% yield (Found: C, 49.59; H, 4.75; N, 5.09; calc. for $C_{24}H_{27}N_2O_4P_2ClAg$: C, 49.55; H, 4.50; N, 4.82%), together with a small amount of plate-like crystals of the solvate **11**·CH_2Cl_2, [Ag_2(μ-L^2)$_2$]-[Ag(L^2)$_2$](ClO_4)$_3$·CH_2Cl_2.

X-Ray crystallography

For each of complexes **2**, **3**, **4**·$2CH_2Cl_2$, **5**, **6**, **9** and **11**·CH_2Cl_2, a selected single crystal was mounted on a Bruker SMART 1000 CCD diffractometer operating at 50 kV and 30 mA using Mo-Kα radiation (0.71073 Å). Data collection and reduction were performed using the SMART and SAINT software,[7] with frames of 0.3° oscillation in the θ range $1.5 < \theta < 28°$ (for **11**·CH_2Cl_2, $\theta < 26°$). An empirical absorption correction was applied using the SADABS program.[8] The data for **1**, **7**·CH_3CN and **8** were collected at 293 K in the variable ω-scan mode on a Siemens R3m/V four-circle diffractometer using Mo-Kα radiation (50 kV, 30 mA; $2\theta_{max} = 52°$). An empirical absorption correction was applied using ψ-scan data. The structures were solved by direct methods and all non-hydrogen atoms were subjected to anisotropic refinement by full-matrix least squares on F^2 using the SHELXTL package.[9] All hydrogen atoms were generated geometrically (C–H bond lengths fixed at 0.96 Å), assigned appropriate isotropic thermal parameters and included in structure factor calculations. Crystal structure data and refinement details are summarised in Table 1.

CCDC reference numbers 171811–171820.

See http://www.rsc.org/suppdata/dt/b1/b109191n/ for crystallographic data in CIF or other electronic format.

Results and discussion

The reactions of *N*-[(diphenylphosphino)methyl]-2-pyridinamine, L^1, and *N*-cyclohexyl-*N*-[(diphenylphosphino)methyl]-2-pyridinamine, L^2, with different metal salts are shown in Scheme 3 and 4, respectively. When L^1 is mixed with $Co(ClO_4)_2$·$6H_2O$ in air, the oxidation state of the phosphorus atom is converted from III to V, and the pyridine ring is protonated to form a perchlorate salt, namely compound **1**. The structure of **1**

Table 1 Crystal data and refinement details for the studied complexes

Complex	**1**	**2**	**3**	**4**·2CH$_2$Cl$_2$	**5**	**6**	**7**·CH$_3$CN	**8**	**9**	**11**·CH$_2$Cl$_2$
Formula	$C_{18}H_{18}ClN_2O_5P$	$C_{39}H_{34}FeN_4O_3P_2$	$C_{36}H_{34}Cl_2N_4O_8P_2Pd$	$C_{38}H_{38}Cl_8N_4P_2Pd_2$	$C_{36}H_{34}ClCuN_4O_4P_2$	$C_{20}H_{20}AgClN_3O_4P$	$C_{43}H_{43}AgClN_7O_4P_2$	$C_{24}H_{27}Cl_2N_2PPd$	$C_{48}H_{54}ClCuN_4O_4P_2$	$C_{97}H_{110}Ag_3Cl_5N_8O_{12}P_4$
M	408.76	724.49	889.91	1109.03	747.60	540.58	927.10	551.75	911.88	2204.67
Crystal system	Monoclinic	Monoclinic	Monoclinic	Triclinic	Orthorhombic	Monoclinic	Triclinic	Monoclinic	Monoclinic	Monoclinic
Space group	$P2_1/n$ (no. 14)	$C2/c$ (no. 15)	$P2_1/n$ (no. 14)	$P\bar{1}$ (no. 2)	$Pca2_1$ (no. 29)	Pn (no. 7)	$P\bar{1}$ (no. 2)	$P2_1/n$ (no. 14)	$P2_1/c$ (no. 14)	$C2$ (no. 5)
Crystal size/mm	0.40 × 0.30 × 0.30	0.45 × 0.25 × 0.18	0.40 × 0.25 × 0.20	0.30 × 0.24 × 0.20	0.60 × 0.40 × 0.40	0.42 × 0.34 × 0.30	0.60 × 0.56 × 0.50	0.54 × 0.42 × 0.40	0.42 × 0.38 × 0.20	0.38 × 0.20 × 0.16
a/Å	12.375(2)	21.007(5)	9.644(2)	9.703(2)	15.255(1)	11.163(3)	11.160(2)	9.21992)	15.0567(8)	21.413(3)
b/Å	9.4683(9)	8.964(2)	21.221(4)	10.229(2)	11.3123(9)	17.485(4)	11.307(2)	20.438(3)	11.0961(6)	9.531(2)
c/Å	16.821(2)	19.136(5)	18.761(3)	12.939(3)	20.678(2)	11.486(3)	17.485(3)	12.965(2)	26.842(1)	26.950(5)
α/°				97.913(5)			92.01(1)			
β/°	97.30(1)	102.400(5)	98.442(4)	103.563(4)		91.452(5)	94.21(2)	105.78(1)	90.723(1)	110.207(4)
γ/°				113.954(4)			104.60(1)			
U/Å^3	1954.9(4)	3519.4(16)	3798.0(12)	1101.0(4)	3568.3(5)	2241.1(10)	2126.2(6)	2350.7(6)	4484.2(4)	5161.7(14)
Z	4	4	4	1	4	4	2	4	4	2
D_c/g cm^{-3}	1.389	1.367	1.556	1.673	1.392	1.602	1.448	1.559	1.351	1.419
F(000)	848	1504	1808	552	1544	1088	952	1120	1912	2260
μ(Mo-Kα)/mm^{-1}	0.309	0.563	0.770	1.408	0.821	1.121	0.663	1.099	0.667	0.815
Total refl.	4952	11336	25481	7548	23691	15446	9709	5765	29874	12559
Unique refl. (R_{int})	3844 (0.0156)	4220 (0.0426)	9136 (0.0281)	5232 (0.0281)	8170 (0.0273)	7140 (0.0416)	8349 (0.0224)	4576 (0.0383)	10772 (0.0573)	9356 (0.0463)
Observed refl.	2706	2786	5578	3574	6619	4771	5597	2855	6253	5844
Parameters	272	223	479	244	434	558	533	272	541	597
Goodness of fit	1.103	0.947	0.919	0.932	0.944	0.950	1.026	0.978	0.913	0.952
$R1$, $wR2$ [$I > 2\sigma(I)$][a]	0.0503, 0.1070	0.0376, 0.0917	0.0426, 0.0909	0.0458, 0.1082	0.0297, 0.0630	0.0503, 0.1345	0.0561, 0.1222	0.0465, 0.0757	0.0485, 0.1112	0.0768, 0.1781
$R1$, $wR2$ (all data)	0.0808, 0.1195	0.0641, 0.1021	0.0842, 0.1115	0.0732, 0.1179	0.0417, 0.0669	0.0800, 0.1489	0.0957, 0.1395	0.1015, 0.0890	0.0919, 0.1286	0.1180, 0.2047

[a] $R1 = \Sigma(|F_o| - |F_c|/\Sigma|F_o|$; $wR2 = \{w[\Sigma(|F_o| - |F_c|)^2]/\Sigma|F_o|^2\}^{1/2}$.

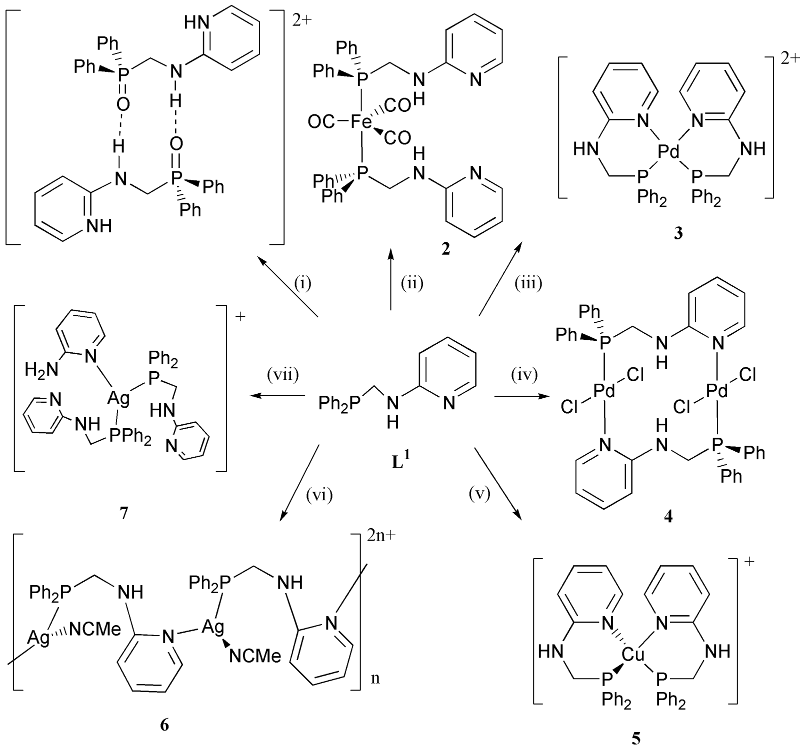

Scheme 3 Reactions of *N*-[(diphenylphosphino)methyl]-2-pyridinamine, L^1. Reagents: (i) $Co(ClO_4)_2·6H_2O$; (ii) $Fe(CO)_5$/KOH; (iii) Na_2PdCl_4/$TlClO_4$; (iv) Na_2PdCl_4; (v) $[Cu(CH_3CN)_4]ClO_4$; (vi) $AgClO_4$; (vii) $AgClO_4$/(2-py)NH_2.

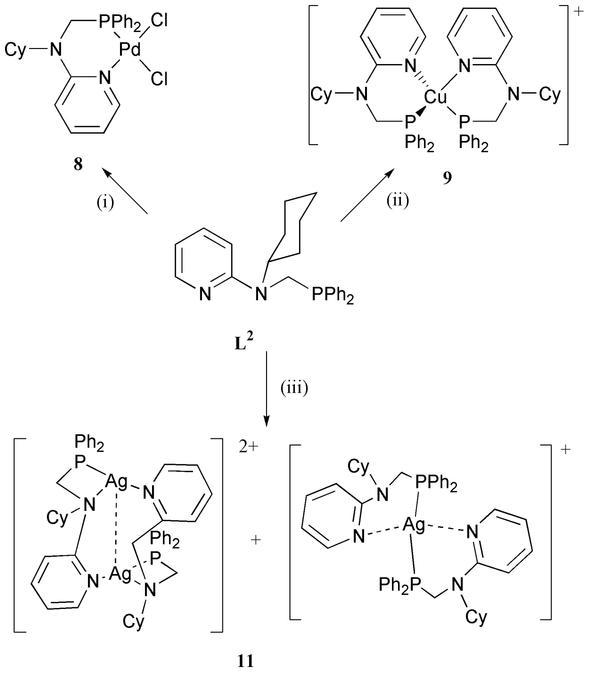

Scheme 4 Reactions of *N*-cyclohexyl-*N*-[(diphenylphosphino)methyl]-2-pyridinamine, L^2. Reagents: (i) Na_2PdCl_4; (ii) $[Cu(CH_3CN)_4]ClO_4$; (iii) $AgClO_4$.

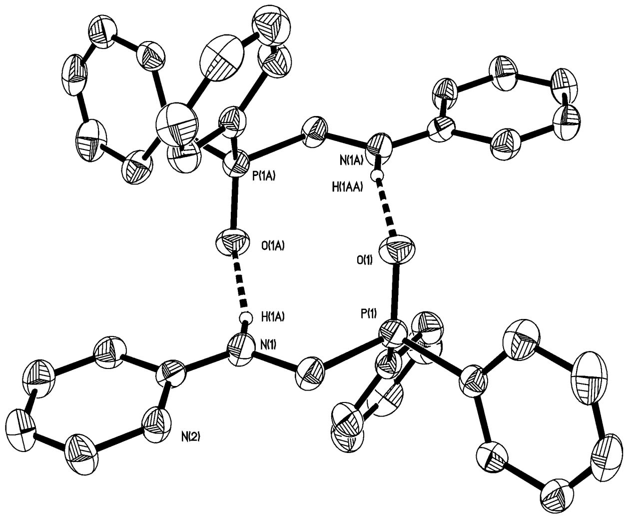

Fig. 1 Perspective drawing (35% thermal ellipsoids) of the cationic dimer in compound **1**. Selected bond lengths (Å) and angles (°): P(1)–O(1) 1.488(2), P(1)–C(1) 1.791(3), P(1)–C(7) 1.798(3), P(1)–C(13) 1.813; O(1)–P(1)–C(1) 113.0(1), O(1)–P(1)–C(7) 112.5(1), O(1)–P(1)–C(13) 112.5(2), C(1)–P(1)–C(7) 108.7(2), C(1)–P(1)–C(13) 106.8(2), C(7)–P(1)–C(13) 102.8(1).

as determined by X-ray crystallography (Fig. 1) confirms the presence of a tertiary phosphine oxide with a P=O bond length of 1.488(2) Å, which is consistent with appreciable double bond character. A pair of cations is linked into a pseudo ten-membered ring dimer through intermolecular P=O ··· H–N hydrogen bonding (O ··· N 2.7, H ··· O 1.956 Å; N–H ··· O 164.7°). Other examples of P=O ··· H–N hydrogen-bonded dimers in $Ph_2P(O)CH_2N(H)C_5H_3N(5\text{-}Cl)$[10a] and $[H\{Ph_2P(O)CH_2(C_4H_8NO)\}]_2(Hg_2I_6)$[10b] have been reported.

The reaction of L^1 or L^2 with KOH and $Fe(CO)_5$ in refluxing ethanol for 24 h gave yellow precipitates formulated as *trans*-$Fe(CO)_3(L^1)_2$, **2** and *trans*-$Fe(CO)_3(L^2)_2$, respectively.[5b] The IR spectra of both complexes have intense carbonyl absorptions at 1880 cm^{-1}, indicating that the local symmetry at the Fe atom is near D_{3h}. In the crystal structure of **2**, a crystallographic C_2 axis bisects the planar $Fe(CO)_3$ unit of the molecule (Fig. 2). The coordination environment about the iron atom is best described as an FeP_2C_3 trigonal bipyramid with the phosphine ligands occupying axial positions. The P–Fe–P angle of 179.44(3)° is comparable to those in *trans*-$Fe(CO)_3(Ph_2Ppym)_2$ [174.2(1)],[11] *trans*-$Fe(CO)_3(Ph_2Ppy)_2$ [177.1(1)]°[3d] and *trans*-$Fe(CO)_3(Ph_2PCH_2mor)_2$ [178.24(3)°][10b] The three C–Fe–C angles [119.5(2), 120.26(8) and 120.26(8)°] are very close to the ideal value of 120°. *trans*-$Fe(CO)_3(\mu\text{-}L^2)_2$ was successfully reacted with $[Cu(CH_3CN)_4]ClO_4$ to form a heterobimetallic seven-membered macrocyclic complex with a Fe(0) ⟶ Cu(I) donor–acceptor bond.[5b] However, the reaction of **2** with copper(I) salts did not

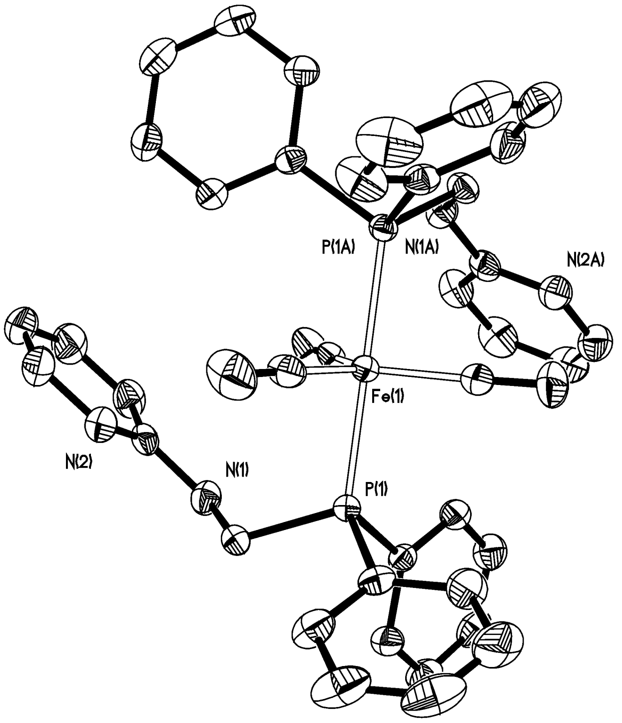

Fig. 2 Perspective drawing (35% thermal ellipsoids) of the molecular structure of **2**. Selected bond lengths (Å) and angles (°): Fe(1)–C(1) 1.781(3), Fe(1)–C(2) 1.766(2), Fe(1)–P(1) 2.1958(6); C(2)–Fe(1)–C(1) 120.26(8), C(2A)–Fe(1)–C(2) 119.5(2), C(1)–Fe(1)–P(1) 89.72(2), C(2)–Fe(1)–P(1) 87.38(7), C(2A)–Fe(1)–P(1) 92.90(7), P(1A)–Fe(1)–P(1) 179.44(3). Symmetry code: −*x*, *y*, 1/2 − *z*.

afford an analogous stable binuclear complex. This seems to be attributable to the greater bulk of L^2 as compared to L^1, since the pyridine ring in L^1 can rotate more freely than that in L^2.

The reaction of L^1 and Na_2PdCl_4 in a 2 : 1 molar ratio in CH_2Cl_2 gave a yellow solution and a NaCl precipitate. When the filtrate was treated with two equivalents of $TlClO_4$ to remove the chloride ligands, the complex $[Pd(L^1)_2](ClO_4)_2$, **3**, was formed. The dication has a near square-planar environment around the Pd center with two *cis* P,N-chelating ligands (Fig. 3). The Pd–P and Pd–N distances are similar to those found in palladium phosphine and pyridylphosphine complexes. The planarity of the coordination geometry around the palladium atom was accessed by fitting a least-squares plane to the atoms Pd(1), P(1), P(2), N2 and N4, which showed a large mean deviation of 0.25 Å. The plane defined by Pd and the coordinated P atoms makes a dihedral angle of 21.9° with the PdN_2 mean plane.

The reaction of L^1 and Na_2PdCl_4 in a 1 : 1 molar ratio in CH_2Cl_2 yielded a yellow solution from which $Pd_2Cl_4(\mu\text{-}L^1)_2\cdot 2CH_2Cl_2$, **4**$\cdot 2CH_2Cl_2$, was isolated. Complex **4** consists of a bimetallic twelve-membered ring located at an inversion center (Fig. 4). The chloride ligands are in a *trans* arrangement about each palladium atom, and a pair of bidentate L^1 ligands in the head-to-tail configuration bridge the two palladium atoms. The Cl(1)–Pd(1)–Cl(2) [174.52(5)] and P–Pd–N [176.6(1)°] angles are close to linear, and the Pd–P [2.252(1)], Pd–N [2.116(4)] and Pd–Cl [2.300(1) and 2.303(1) Å] bond distances are quite normal. The least-squares plane through the atoms Pd(1), Cl(1), Cl(2), P(1) and N(1A) has a mean deviation of 0.05 Å. The dihedral angle between the plane Pd(1)–Cl(1)–Cl(2)–P(1)–N(1A) and the pyridine ring is 74.5°. The non-bonded Pd ··· Pd separation in this compound is 4.594 Å, which is slightly shorter than that in twelve-membered ring dipalladium complexes linked by a rigid phosphine ligand (4.710 Å).[12]

The complex $[Cu(L^1)_2]ClO_4$, **5**, was obtained from the reaction of L^1 with $[Cu(CH_3CN)_4]ClO_4$ in a 2 : 1 molar ratio in $CH_3CN\text{–}CH_2Cl_2$. The structure of the cation is shown in Fig. 5.

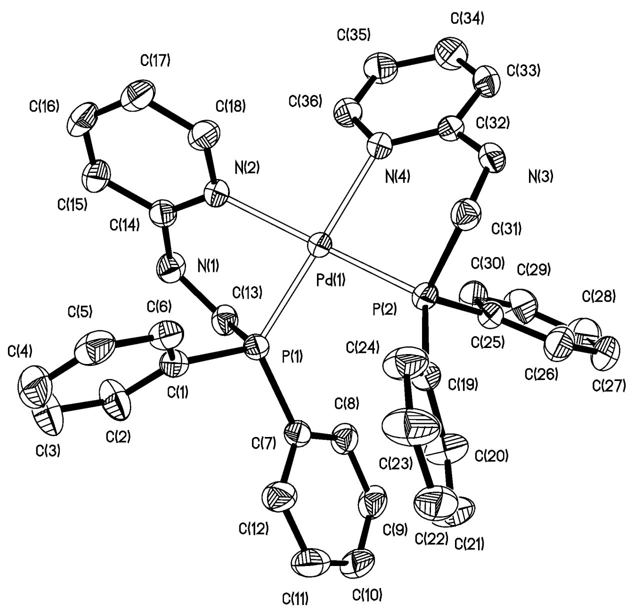

Fig. 3 Perspective drawing (35% thermal ellipsoids) of the dication in compound **3**. Selected bond lengths (Å) and angles (°): Pd(1)–N(2) 2.131(3), Pd(1)–N(4) 2.175(3), Pd(1)–P(1) 2.231(1), Pd(1)–P(2) 2.235(1), N(2)–Pd(1)–N(4) 93.1(1); N(2)–Pd(1)–P(1) 83.83(8), N(4)–Pd(1)–P(1) 161.05(9), N(2)–Pd(1)–P(2) 166.22(9), N(4)–Pd(1)–P(2) 89.09(8), P(1)–Pd(1)–P(2) 98.37(4).

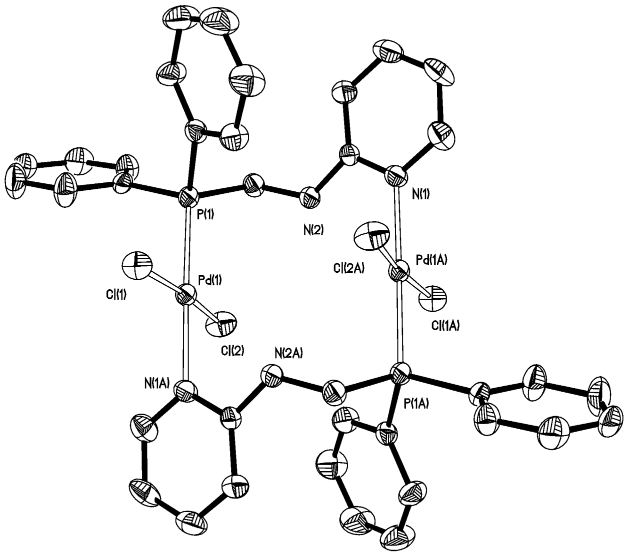

Fig. 4 Perspective drawing (35% thermal ellipsoids) of the dinuclear molecule of **4** in **4**$\cdot 2CH_2Cl_2$. Selected bond lengths (Å) and angles (°): Pd(1)–N(1A) 2.116(4), Pd(1)–P(1) 2.252(1), Pd(1)–Cl(2) 2.300(1), Pd(1)–Cl(1) 2.303(1); N(1A)–Pd(1)–P(1) 176.6(1), N(1A)–Pd(1)–Cl(2) 88.3(1), P(1)–Pd(1)–Cl(2) 88.26(5), N(1A)–Pd(1)–Cl(1) 90.2(1), P(1)–Pd(1)–Cl(1) 93.29(5), Cl(2)–Pd(1)–Cl(1) 174.52(5). Symmetry code: 1 − *x*, 1 − *y*, 1 − *z*.

The copper atom has a distorted tetrahedral geometry, in which each L^1 ligand chelates the metal center through its phosphorus and pyridyl nitrogen atoms. The Cu–P [2.2282(6) and 2.2353(6)] and Cu–N [2.113(2) and 2.171(2) Å] bond lengths fall within the normal ranges for copper phosphine and pyridine complexes. The bond angles at the copper atom vary from 94.58(7) to 128.74(3)°.

The reaction of L^1 with silver perchlorate in a 1 : 1 molar ratio in $CH_3CN\text{–}CH_2Cl_2$ leads to rapid formation of a colorless solution, from which $[Ag(CH_3CN)(\mu\text{-}L^1)]_n(ClO_4)_n$, **6**, was isolated. The ligand L^1 bridges consecutive metal centers *via* its P,N(pyridyl)-donor sites. Each of the two independent silver centers is coordinated by a P atom from one L^1 ligand and a pyridyl N atom from another, resulting in the formation of a

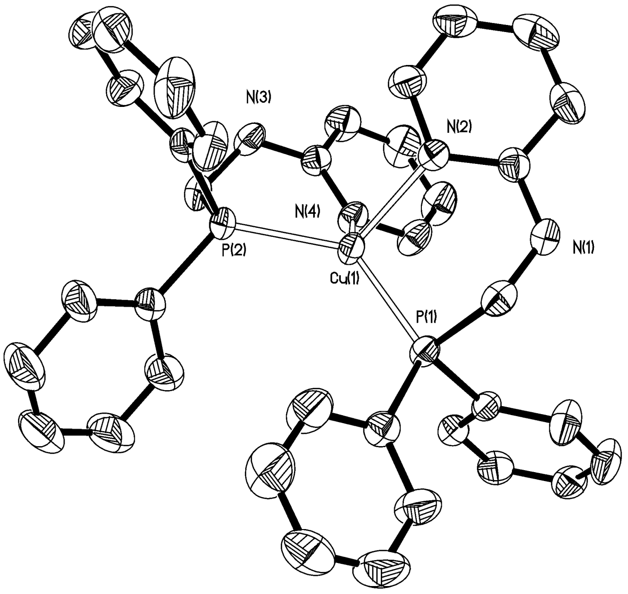

Fig. 5 Perspective drawing (35% thermal ellipsoids) of the cation in compound **5**. Selected bond lengths (Å) and angles (°): Cu(1)–N(2) 2.171(2), Cu(1)–N(4) 2.113(2), Cu(1)–P(1) 2.2282(6), Cu(1)–P(2) 2.2353(6); N(4)–Cu(1)–N(2) 94.58(7), N(4)–Cu(1)–P(1) 120.45(5), N(2)–Cu(1)–P(1) 96.37(5), N(4)–Cu(1)–P(2) 96.89(5), N(2)–Cu(1)–P(2) 115.61(5), P(1)–Cu(1)–P(2) 128.74(3).

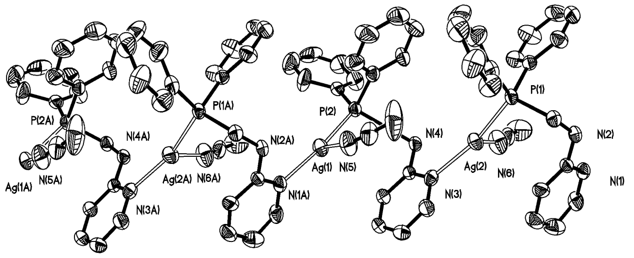

Fig. 6 Structure of the polymeric chain $[Ag_2(CH_3CN)_2(\mu\text{-}L^1)_2]_n^{2n+}$ in **6**. Selected bond lengths (Å) and angles (°): Ag(1)–N(1A) 2.185(7), Ag(1)–P(2) 2.359(2), Ag(1)–N(5) 2.60(1), Ag(2)–N(3) 2.193(8), Ag(2)–P(1) 2.369(2), Ag(2)–N(6) 2.55(1); N(1A)–Ag(1)–P(2) 166.0(2), N(1A)–Ag(1)–N(5) 92.1(3), P(2)–Ag(1)–N(5) 101.7(2), N(3)–Ag(2)–P(1) 159.1(2), N(3)–Ag(2)–N(6) 94.6(3), P(1)–Ag(2)–N(6) 105.4(3). Symmetry code: *x*, *y*, *z* − 1.

cationic polymeric chain running in the direction of the *c* axis (Fig. 6). The highly distorted trigonal planar coordination environment about each Ag(I) atom is completed by a CH_3CN ligand, with a slightly longer Ag–N bond [2.60(1) and 2.55(1) Å] that stabilises the resulting 16-electron configuration. The three bond angles at Ag(1) and Ag(2) sum to 359.8 and 359.2°, respectively. The non-bonded Ag ··· Ag separations in the polymeric chain are 5.827 and 6.019 Å, respectively. The crystal structure of **6** consists of the packing of such chains and the perchlorate ions.

The reaction of L^1 with $AgClO_4$ in a 2 : 1 molar ratio in the presence of 2-aminopyridine afforded the mononuclear complex $[Ag(L^1)_2(2\text{-Py–NH}_2)]ClO_4$, **7** (Fig. 7). The silver atom in **7** is coordinated by two L^1 ligands and one 2-aminopyridine, with fairly normal Ag–P and Ag–N bond lengths. The three P(1)–Ag(1)–N(6), P(2)–Ag(1)–N(6) and P(1)–Ag(1)–P(2) [119.1(1), 112.9(1) and 127.99(5)°] bond angles are not far from the ideal value of 120°, which indicates trigonal planar coordination geometry at the silver atom.

The reaction of *N*-cyclohexyl-*N*-[(diphenylphosphino)-methyl]-2-pyridinamine, L^2, with Na_2PdCl_4 in a 1 : 1 molar ratio gave a yellow solution from which the complex $PdCl_2(L^2)$, **8**, was isolated. The L^2 ligand chelates the palladium atom through its P and pyridyl N atoms, with two chloride ligands arranged in *cis* positions (Fig. 8). The Pd–P and Pd–N distances are similar to those seen in palladium phosphine and pyridylphosphine complexes. The least-squares plane through the atoms Pd(1), P(1), N(1), Cl(1) and Cl(2) shows a mean deviation of 0.09 Å. The configuration at the tertiary amino nitrogen atom is almost planar, as its deviation from the plane of its three-bonded carbon atoms is 0.22 Å. The dihedral angle of this plane and the pyridine ring is 27.4°, which indicates that the lone pair electron of the tertiary amino nitrogen atom is significantly conjugated with the pyridine ring.

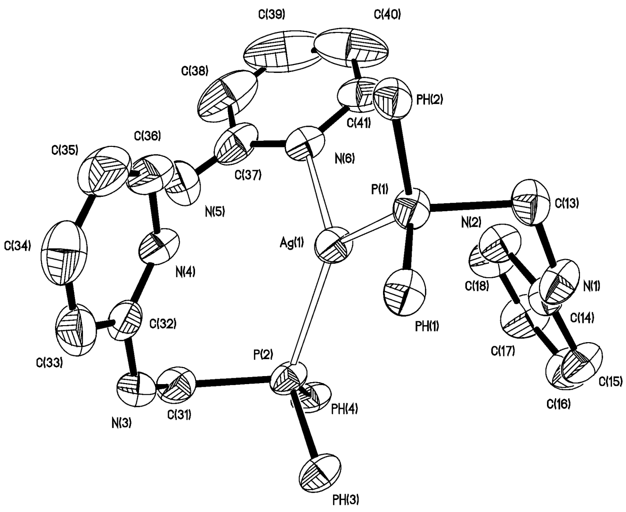

Fig. 7 Perspective drawing (35% thermal ellipsoids) of the cation in compound $\mathbf{7}\cdot CH_3CN$. Selected bond lengths (Å) and angles (°): Ag(1)–N(6) 2.350(4), Ag(1)–P(1) 2.437(1), Ag(1)–P(2) 2.448(1); N(6)–Ag(1)–P(1) 119.1(1), N(6)–Ag(1)–P(2) 112.9(1), P(1)–Ag(1)–P(2) 127.99(5).

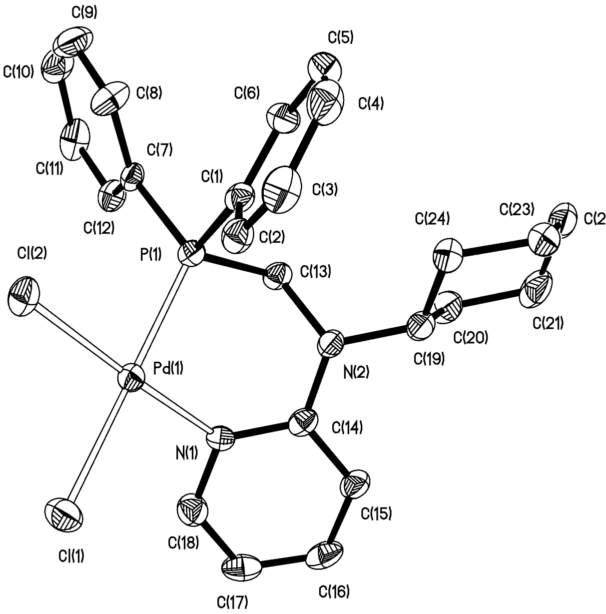

Fig. 8 Perspective drawing (35% thermal ellipsoids) of the molecular structure of compound **8**. Selected bond lengths (Å) and angles (°): Pd(1)–N(1) 2.105(4), Pd(1)–P(1) 2.192(1), Pd(1)–Cl(2) 2.290(1), Pd(1)–Cl(1) 2.405(1); N(1)–Pd(1)–P(1) 92.5(1), N(1)–Pd(1)–Cl(2) 174.0(1), P(1)–Pd(1)–Cl(2) 84.02(5), N(1)–Pd(1)–Cl(1) 92.5(1), P(1)–Pd(1)–Cl(1) 171.78(6), Cl(2)–Pd(1)–Cl(1) 91.60(5).

The compound $[Cu(L^2)_2]ClO_4$, **9**, was obtained from the reaction of L^2 with $[Cu(CH_3CN)_4]ClO_4$ in a 2 : 1 molar ratio in CH_2Cl_2. The structure of the cation is shown in Fig. 9. The copper atom has a distorted tetrahedral geometry, in which each L^2 ligand chelates the metal center through its phosphorus atom and nitrogen atom in the pyridine ring. The Cu–P [2.2086(7) and 2.2279(7)] and Cu–N [2.107(2) and 2.181(2) Å] bond lengths fall within the normal bond ranges for copper phosphine and pyridine complexes. The bond angles at the

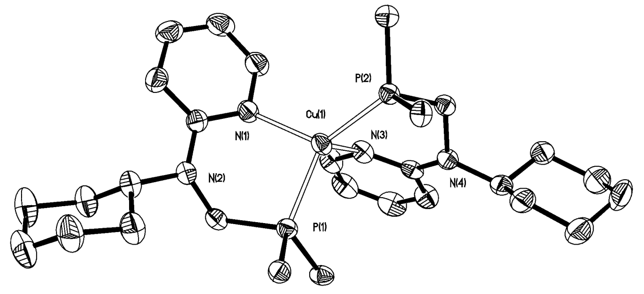

Fig. 9 Perspective drawing (35% thermal ellipsoids) of the cation in compound **9**. Selected bond lengths (Å) and angles (°): Cu(1)–N(1) 2.107(2), Cu(1)–N(3) 2.181(2), Cu(1)–P(2) 2.2086(7), Cu(1)–P(1) 2.2279(7); N(1)–Cu(1)–N(3) 99.18(9), N(1)–Cu(1)–P(2) 123.96(7), N(3)–Cu(1)–P(2) 94.58(6), N(1)–Cu(1)–P(1) 95.04(6), N(3)–Cu(1)–P(1) 104.13(6), P(2)–Cu(1)–P(1) 133.34(3).

copper atom vary from 94.58(6) to 133.34(3)°. The configuration at the tertiary amino nitrogen atom is nearly planar, with its lone pair electrons fully conjugated with the pyridine ring.

The reaction of L^2 with $AgClO_4$ in a 1 : 1 molar ratio in $CH_3CN–CH_2Cl_2$ affords needle-like microcrystals of **10**, of stoichiometry $Ag(L^2)ClO_4$ by elemental analysis, plus a small quantity of plate-like crystals, which were subsequently shown by X-ray analysis to be a solvate with the structural formula $[Ag_2(\mu-L^2)_2][Ag(L^2)_2](ClO_4)_3·CH_2Cl_2$, **11**·$CH_2Cl_2$. The $[Ag_2(\mu-L^2)_2]^{2+}$ dication has crystallographic C_2 symmetry with a pair of P,N(pyridyl)-bidentate L^2 ligands bridging the silver atoms in a head-to-tail fashion (Fig. 10). Notably, the tertiary amino N atom of each L^2 is coordinated to a silver atom with Ag–N = 2.603(9) Å. This distance is longer than those in silver tertiary amine complexes, but shorter than the sum of the van der Waals' radii of silver and nitrogen atoms. Furthermore, the amino nitrogen atom is displaced by 0.39 Å from the plane of its three-bonded carbon atoms, and the dihedral angle of this plane and the pyridine ring (99.9°) is much larger than those in complexes **8**, **9** and the cation $[Ag(L^2)_2]^+$ in **11**·CH_2Cl_2. This means that its lone pair electrons are no longer conjugated with the pyridine ring, but involved in coordination with the silver atom, although the binding is rather weak. The Ag–P and Ag–N(pyridyl) bonds fall in the normal ranges for silver phosphine and pyridine complexes. In this dimeric cation, the Ag ··· Ag distance of 2.890(2) Å is comparable to twice the metallic radius of silver (2.89 Å) and the corresponding values of 2.934(2) and 2.946(2) Å in $[Ag_2(H_2L)_3]_n^{2n+}$ [H_2L = *N*′,*N*′-bis(salicylidene)-1,4-diaminobutane],[13a] 2.936(1)–2.960(1) Å in $[Ag_2(\mu-dcpm)_2]^+$ [dcpm = bis(dicyclohexylphosphino)methane],[13b] 2.7–3.0 Å in polyhedral silver cages each encapsulating a C_2^{2-} anion ($C_2@Ag_n$, n = 6, 7, 8, 9)[13d] and 2.953(2)–2.986(2) Å in the silver alkynyl cage compounds $[Ag_{14}(\mu-C{\equiv}C–tBu)_{12}X]Y$ (X = Cl, Br; Y = OH, BF_4).[13e] These distances are suggestive of significant argentophilic interaction between the silver(I) centers,[13] so this type of metallophilic $d^{10}–d^{10}$ interaction also exists in the present dication, and the coordination geometry at each silver atom can be described as highly distorted tetrahedral (Fig. 10).

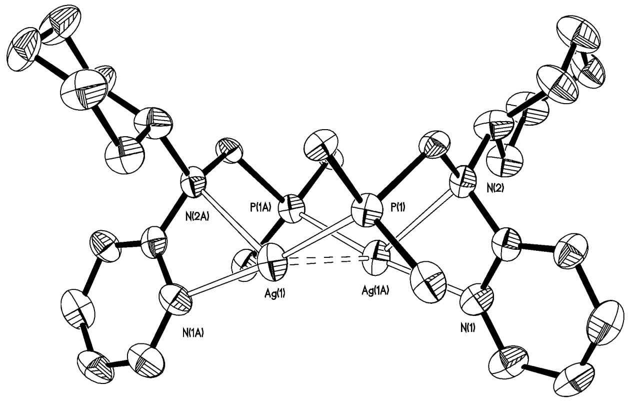

Fig. 10 Perspective drawing (35% thermal ellipsoids) of the dinuclear cation $[Ag_2(\mu-L^2)_2]^{2+}$ in compound **11**·CH_2Cl_2. Selected bond lengths (Å) and angles (°): Ag(1)–N(1A) 2.252(9), Ag(1)–P(1) 2.372(3), Ag(1)–N(2A) 2.603(8), Ag(1)–Ag(1A) 2.890(2); N(1A)–Ag(1)–P(1) 169.7(2), N(1A)–Ag(1)–N(2A) 54.6(3), P(1)–Ag(1)–N(2A) 122.7(2), N(1A)–Ag(1)–Ag(1A) 100.9(2), P(1)–Ag(1)–Ag(1A) 88.60(7), N(2A)–Ag(1)–Ag(1A) 87.9(2). Symmetry code: $-x + 1, y, -z$.

An ORTEP drawing of the cation $[Ag(L^2)_2]^+$ in **11**·CH_2Cl_2 is shown in Fig. 11. A crystallographic C_2 axis bisects the molecule through the silver atom, which is coordinated by two equivalent phosphine ligands with Ag–P = 2.388(2) Å and P–Ag–P = 164.8(2)°. The distance (2.647 Å) between the silver atom and each pyridyl nitrogen atom is much longer than those in known silver pyridine complexes, which means that only a feeble interaction exists between them.

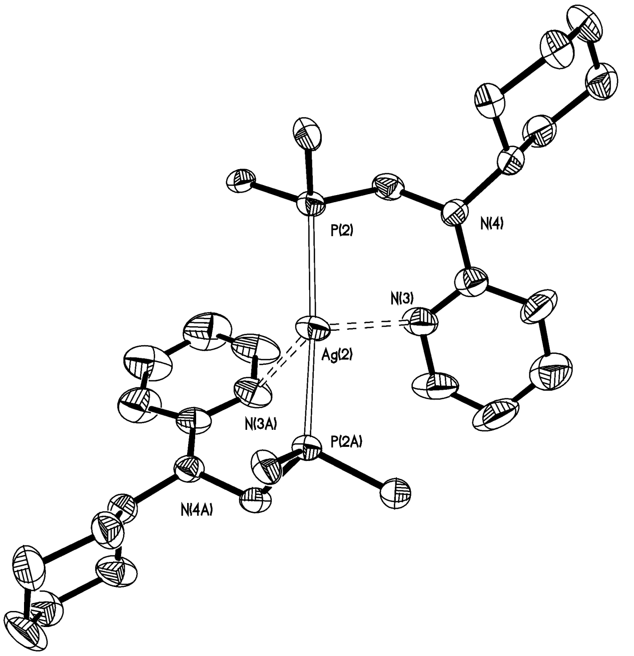

Fig. 11 Perspective drawing (35% thermal ellipsoids) of the cation $[Ag(L^2)_2]^+$ in compound **11**·CH_2Cl_2. Selected bond lengths (Å) and angles (°): Ag(2)–P(2) 2.388(2); P(2)–Ag(2)–P(2A) 164.8(2). Symmetry code: $1 - x, y, 1 - z$.

Conclusion

Two functionalised amine ligands, *N*-[(diphenylphosphino)-methyl]-2-pyridinamine (L^1) and *N*-cyclohexyl-*N*-[(diphenylphosphino)methyl]-2-pyridinamine (L^2), have been reacted with $Fe(CO)_5$ and palladium(II), copper(I) and silver(I) salts in different molar ratios to generate a series of complexes exhibiting a variety of new ligation modes: P-coordination (**a**), P,N(pyridyl)-chelating (**d**) and P,N(pyridyl)-bridging (**h**) for L^1; P,N(pyridyl)-chelating (**d**) and a novel P,N(amine),-N(pyridyl)-bridging mode (**l**) for L^2. Although there are thirteen conceivable coordination modes for this kind of phosphinopyridinamine ligand, those that involve the weakly coordinating and sterically hindered amino N atom seem unlikely to be observed in metal complexes, and argentophilicity appears to play a significant role in inducing the adoption of the tridentate mode **l** in $[Ag_2(\mu-L^2)_2]^{2+}$.

Acknowledgements

This work is supported by Hong Kong Research Grants Council Earmarked Grant CUHK 4022/98.

References

1 See, for example: (*a*) J. C. Jeffrey and T. B. Rauchfuss, *Inorg. Chem.*, 1979, **18**, 2658; (*b*) E. T. Singewald, C. A. Mirkin and C. L. Stern, *Angew. Chem., Int. Ed. Engl.*, 1995, **34**, 1624; (*c*) E. Valls, J. Suades, B. Donadieu and R. Mathieu, *Chem. Commun.*, 1996, 771; (*d*) C. S. Slone, C. A. Mirkin, G. P. A. Yap, I. A. Guzei and A. L. Rheingold, *J. Am. Chem. Soc.*, 1997, **119**, 10743; (*e*) C. W. Rogers and M. O. Wolf, *Chem. Commun.*, 1999, 2297; (*f*) I. D. Kostas, *J. Organomet. Chem.*, 2001, **626**, 221; (*g*) F. Emmenegger, C. W. Schlaepfer, H. Stoeckli-Evans, M. Piccand and H. Piekarski, *Inorg. Chem.*, 2001, **40**, 3884.

2 See, for example: (*a*) G. R. Newcome, *Chem. Rev.*, 1993, **93**, 2067; (*b*) H. Cheng and Z.-Z. Zhang, *Coord. Chem. Rev.*, 1996, **147**, 1; (*c*) P. Espinet and K. Soulantica, *Coord. Chem. Rev.*, 1999, **195**, 499; (*d*) S.-M. Kuang, Z.-Z. Zhang, Q.-G. Wang and T. C. W. Mak, *Inorg. Chem.*, 1998, **37**, 6090; (*e*) H.-B. Song, Z.-Z. Zhang and T. C. W. Mak, *Inorg. Chem.*, 2001, **40**, 5928.

3 See, for example: (*a*) J. P. Farr, M. M. Olmatead and A. L. Balch, *J. Am. Chem. Soc.*, 1980, **102**, 6654; (*b*) P. Braunstein, D. G. Kelly, A. Tiripicchio and F. Ugozzoli, *Bull. Soc. Chim. Fr.*, 1995, **132**, 1083; (*c*) S.-M. Kuang, H. Cheng, L.-J. Sun, Z.-Z. Zhang, Z.-Y. Zhou, B.-M. Wu and T. C. W. Mak, *Polyhedron*, 1996, **15**, 3417; (*d*) S.-L. Li, T. C. W. Mak and Z.-Z. Zhang, *J. Chem. Soc., Dalton Trans*, 1996, 3475; (*e*) Z.-Z. Zhang, H. Cheng, S.-M. Kuang, Y.-Q. Zhou, Z.-X. Liu, J.-K. Zhang and H.-G. Wang, *J. Organomet. Chem.*, 1996, **516**, 1; (*f*) S.-M. Kuang, F. Xue, C.-Y. Duan, T. C. W. Mak and Z.-Z. Zhang, *J. Organomet. Chem.*, 1997, **534**, 15; (*g*) S.-M. Kuang, Z.-Z. Zhang, B.-M. Wu, T. C. W. Mak and Z.-Z. Zhang, *J. Organomet. Chem.*, 1997, **540**, 55; (*h*) S.-M. Kuang, F. Xue, T. C. W. Mak and Z.-Z. Zhang, *Inorg. Chim. Acta*, 1999, **284**, 119; (*i*) V. J. Catalano, B. L. Bennett, S. Muratidis and B. C. Noll, *J. Am. Chem. Soc.*, 2001, **123**, 173.

4 (*a*) S. J. Berners-Price, R. J. Bowen, P. Galettis, P. C. Healy and M. J. Mckeage, *Coord. Chem. Rev.*, 1999, **186**, 823; (*b*) C. Hahn, A. Vitagliano, F. Giordano and R. Taube, *Organometallics*, 1998, **17**, 2060; (*c*) P. Wehaman, R. E. Rulke, V. E. Kaasjager, P. C. J. Kamer, H. Kooijman, A. L. Spek, C. J. Elsevier, K. Vrieze and P. W. N. M. Vanleeuwen, *J. Chem. Soc., Chem. Commun.*, 1995, 331; (*d*) M. Driess, F. Franke and K. Merz, *Eur. J. Inorg. Chem.*, 2001, 2661; (*e*) M. J. Green, K. J. Cavell and P. G. Edwards, *J. Chem. Soc., Dalton Trans.*, 2000, 853; (*f*) E. Drent, P. Arnoldy and P. H. M. Budzelaar, *J. Organomet. Chem.*, 1993, **444**, 247; (*g*) E. Drent, P. Arnoldy and P. H. M. Budzelaar, *J. Organomet. Chem.*, 1994, **475**, 57; (*h*) P. C. J. Kamer and P. W. N. M. V. Leeuwen, in *Aqueous-Phase Oranometallic Catalysis: Concepts and Applications*; ed. B. Cornils and W. A. Herrmann, Wiley-VCH, Weinheim, 1998, pp. 564–576; (*i*) C. G. Arena, F. Faraone, M. Lanfranchi, E. Rotondo and A. Tirpicchio, *Inorg. Chem.*, 1992, **31**, 4797; (*j*) A. S. C. Chan, C.-C. Chen, R. Cao, M.-R. Lee, S.-M. Peng and G. H. Lee, *Organometallics*, 1997, **16**, 3469.

5 (*a*) S. E. Durran, M. B. Smith, A. M. Z. Slawin and J. W. Steed, *J. Chem. Soc., Dalton Trans.*, 2000, 2778; (*b*) D.-J. Cui, Q.-S. Li, F.-B. Xu, X.-B. Leng and Z.-Z. Zhang, *Organometallics*, 2001, **20**, 4126.

6 J. J. Brunet, R. Chauvin, O. Diallo, F. Kindela, P. Leglaye and D. Neibecker, *Coord. Chem. Rev.*, 1998, **180**, 331 and reference therein.

7 SMART 5.0 and SAINT 4.0 for Windows NT, Area Detector Control and Integration Software, Bruker Analytical X-Ray Systems, Inc., Madison, WI, USA, 1998.

8 G. M. Sheldrick, SADABS, Program for Empirical Absorption Correction of Area Detector Data, Univ. of Göttingen, Germany, 1996.

9 G. M. Sheldrick, SHELXTL 5.10 for Windows NT, Structure Determination Software, Bruker Analytical X-Ray Systems, Inc., Madison, WI, USA, 1997.

10 (*a*) S. J. Coles, S. E. Durran, M. B. Hursthouse, A. M. Z. Slawin and M. B. Smith, *New J. Chem.*, 2001, **25**, 416; (*b*) H.-B. Song, Q.-M. Wang, Z.-Z. Zhang and T. C. W. Mak, *J. Organomet. Chem.*, 2000, **605**, 15.

11 S.-L. Li, Z.-Z. Zhang and T. C. W. Mak, *J. Organomet. Chem.*, 1997, **537**, 73.

12 S. L. Schiavo, G. De Munno, F. Nicola and G. Tresoldi, *J. Chem. Soc., Dalton Trans.*, 1994, 3125.

13 (*a*) M.-L. Tong, X.-M. Chen, B.-H. Ye and L.-N. Ji, *Angew. Chem., Int. Ed.*, 1999, **38**, 2237; (*b*) C.-M. Che, M.-C. Tse, M. C. W. Chan, K.-K. Cheung, D. L. Phillips and K. H. Leung, *J. Am. Chem. Soc.*, 2000, **122**, 2464; (*c*) M. A. Rawashdeh-Omary, M. A. Omary and H. H. Patterson, *J. Am. Chem. Soc.*, 2000, **122**, 10371; (*d*) Q.-M. Wang and T. C. W. Mak, *Chem. Commun.*, 2001, 807 and references therein; (*e*) D. Rais, J. Yau, D. M. P. Mingos, R. Vilar, A. J. P. White and D. J. Williams, *Angew. Chem., Int. Ed.*, 2001, **40**, 3464; (*f*) P. Pyykkö, *Chem. Rev.*, 1997, **97**, 587.